Hydrogen as an Indicator to Assess Biological Activity During Trace-Metal Bioremediation
Final Report - December 2004
(U.S. Department of Energy, NABIR, Award # DE FG02-00ER1263031)

Peter Jaffé (P.I.), Princeton University
Derek Lovley (Collaborator), University of Massachusetts
John Komlos, Derick Brown, Princeton University

Summary

Trace-metal and/or radionuclide bioremediation schemes require that specific redox conditions be achieved at given zones of an aquifer. Tools are therefore needed to identify the terminal electron acceptor processes (TEAPs) that are being achieved during bioremediation in an aquifer. Dissolved hydrogen (H_2) concentrations have been shown to correlate with specific TEAPs during bioremediation in an aquifer. Theoretical analysis has shown that these steady-state H_2 levels are solely dependent upon the physiological parameters of the hydrogen-consuming microorganisms, with H_2 concentrations increasing as each successive TEAP yields less energy for bacterial growth. The objective of this research was to determine if H_2 can still be used as an indicator of TEAPs during a uranium bioremediation scheme where an organic substrate is injected into the subsurface and organisms may consume H_2 and carbon simultaneously. In addition, the effect of iron bioavailability on H_2 concentrations during iron reduction was observed.

The first phase of research determined the effect of a competing electron donor (acetate) on the kinetics of H_2 utilization by *Geobacter sulfurreducens* in batch cultures under iron reducing conditions. The results indicate that, though the Monod kinetic coefficients describing the rate of H_2 utilization under iron-reducing conditions correlate energetically with the coefficients found in previous experiments under methanogenic and sulfate-reducing conditions, conventionally measured growth kinetics do not predict the steady state H_2 levels typical for each TEAP. In addition, with acetate and H_2 as simultaneous electron donors, there is slight inhibition between the two electron donors for *G. sulfurreducens*, and this can be modeled through competitive inhibition terms in the classic Monod formulation, resulting in slightly higher H_2 concentrations under steady state conditions in the presence of acetate. This dual-donor model indicates that the steady state H_2 concentration in the presence of an organic as electron donor is not only dependent on the biokinetic coefficients of the TEAP, but also the concentration of the organic substrate, and that the H_2 concentration does not start to change very dramatically as long as the organic substrate concentration remains below the half saturation constant. The results for this phase of research are provided in Section 1.

The second phase of research measured steady-state H_2 concentrations under iron reducing conditions using NABIR Field Research Center background soil in a simulated bioremediation scenario involving acetate injection to stimulate indigenous microbial activity in a flow-through column. Steady-state H_2 concentrations measured during this

long-term (500 day) column experiment were higher than observed for iron-reducing conditions in the field even though evidence suggests that iron reduction was the dominant TEAP in the column. Additional column experiments were performed to determine the effect of iron bioavailability on steady-state H_2 concentrations using the humics analogue, AQDS (9,10-anthraquinone-2,6-disulfonic acid). The iron reduction rate in the column with AQDS was double the rate in a parallel column without AQDS and lower steady state H_2 levels were observed in the presence of AQDS, indicating that even though iron reduction does occur, a decreased bioavailability of iron may inhibit iron reduction such that H_2 concentrations increase to levels that are more typical for less energetically favorable reactions (sulfate-reduction, methanogenigesis). The results for this phase of research are in Section 2.

A final phase of research measured the effect of carbon concentration and iron bioavailability on surface bound iron reduction kinetics and steady-state H_2 levels using synthetic iron oxide coated sand (IOCS). Results show a significant decrease in the microbial iron reduction and acetate oxidation rates for systems with surface bound Fe(III) (IOCS) compared to soluble Fe(III) (ferric citrate). The addition of AQDS did not affect the rate of iron reduction for soluble Fe(III) but did increase the rate of surface bound Fe(III) reduction to values similar to soluble Fe(III). IOCS column experiments will be performed using acetate concentration ranges above and below the half saturation constant calculated from the batch experiments to verify if steady-state H_2 concentrations vary with change in carbon concentration as predicted from the dual-donor modeling in phase 1. These results will determine if, and at what concentration, a carbon source added as an electron donor during a biostimulation scenario will compete with H_2 as a co-electron donor and how this interaction will influence the use of H_2 as an indicator of TEAP during bioremediation in an aquifer. The results for this phase of research are in Section 3.

H_2 concentration ranges have been shown to correlate with different TEAP in subsurface environments. The results from this research indicate that this correlation between H_2 concentrations and redox conditions is not only based on the physiological parameters of the hydrogen-consuming microorganisms, but also is affected by such variables as electron acceptor bioavailability, co-electron donor (carbon) concentration and temperature. Though H_2 measurements are still an important tool in the characterization of redox processes during a bioremediation scenario, additional subsurface measurements are essential for an overall understanding of the active TEAP and how these processes influence contaminant bioremediation.

1. Simultaneous Utilization of Acetate and Hydrogen by *Geobacter sulfurreducens*.

Introduction

Modification of TEAPs through injection of an electron donor, such as acetate, has shown promise as a viable method for the immobilization of trace metals and radionuclides in the subsurface at DOE NABIR contamination sites (Anderson et al. 2003; Istok et al. 2004). Monitoring of the TEAP, such as through aqueous hydrogen

concentrations, as electron donor is added is vital to the successful implementation of this technique. However, as there is limited data on H_2 kinetics during the reduction of trace metals, it is unknown how the addition of a competing electron donor will affect the rate of H_2 consumption and how the competing electron donor may affect the observed correlation of H_2 concentration with TEAP.

This research examined the effects of simultaneous hydrogen and acetate utilization through obtaining kinetic parameters under iron-reducing conditions in batch experiments to explore how the presence of an additional electron donor may affect the utilization of hydrogen, and hence the steady-state aqueous hydrogen concentrations. Soluble iron(III)-citrate was used as the electron acceptor rather than solid iron(III)-oxides to avoid surface-bound iron bioavailability limitations in order to focus on the effects of acetate on hydrogen kinetics during iron reduction. *Geobacter sulfurreducens*, an obligate anaerobic bacterium, was used in this study for its ability to reduce iron with either acetate or hydrogen, but not citrate, as electron donors (Coccavo et al. 1994). In addition, *G. sulfurreducens* was chosen because microorganisms with 16S rDNA sequences closely related to *G. sulfurreducens* are the predominant organisms in a variety of subsurface environments in which Fe^{3+} reduction is the predominant TEAP (Lovley 2000; Snoeyenbos-West et al. 2000).

The objectives of this research were to (a) determine kinetic parameters for microbial utilization of hydrogen under iron-reducing conditions and place these values in context of existing parameters for sulfate-reducing and methanogenic conditions; (b) determine kinetic parameters for simultaneous utilization of hydrogen and acetate under iron-reducing conditions; and (c) use these kinetic parameters with a multi-substrate biodegradation model that was formulated to describe the dual-electron donor utilization in order to determine the effects of an organic substrate on steady-state hydrogen concentrations.

Theoretical Considerations

Single-Electron Donor H_2 Kinetics. The concept of dissolved hydrogen (H_2) serving as an indicator to predict the predominant TEAP in sediments resulted from the empirical observation that aquatic sediments with the same predominant TEAP had similar concentrations of dissolved hydrogen and that different TEAPs had distinct ranges of hydrogen concentrations associated with them. This observation was originally explained with a relatively simple model in which it was assumed that the uptake of hydrogen by a particular form of respiration follows Michaelis-Menten type kinetics, thus producing an equation for the steady-state hydrogen concentration that is independent of the rate of hydrogen production and solely dependent upon the physiological parameters of the hydrogen-consuming microorganisms (Lovley and Goodwin, 1988). For example, Michaelis-Menten kinetics for steady-state bacterial concentration, where bacterial growth is balanced by endogenous decay, can be written as:

$$\frac{dX}{dt} = 0 = Y_{\frac{cell}{H_2}} V_{max}^{H_2} \frac{C_{H_2}}{K_M^{H_2} + C_{H_2}} X - bX \qquad (1)$$

where X is the biomass concentration (# cells/mL); C_{H_2} is the aqueous hydrogen concentration (moles/L); $K_m^{H_2}$ is the hydrogen half-saturation constant (moles/L); $V_{max}^{H_2}$ is the maximum rate of hydrogen uptake (moles H_2/# cells/time); $Y_{\frac{cell}{H_2}}$ is the yield coefficient, (# cells/mole H_2); and b is the biomass endogenous decay coefficient (time^{-1}). Solving for the hydrogen concentration gives

$$C_{H_2} = \frac{bK_M^{H_2}}{Y_{\frac{cell}{H_2}} V_{max}^{H_2} - b} \tag{2a}$$

Similarly, for Monod kinetics, the steady-state hydrogen concentration is found to be

$$C_{H_2} = \frac{bK_S^{H_2}}{\mu_{max}^{H_2} - b} \tag{2b}$$

where $K_S^{H_2}$ is the hydrogen half-saturation constant (moles/L) and $\mu_{max}^{H_2}$ is the maximum specific growth rate with hydrogen as the electron donor (time^{-1}). Thus, for the case of a pure culture with hydrogen as the sole electron donor, the hydrogen concentration that provides a steady-state biomass concentration can be determined via Eqn. 2. The parameters $V_{max}^{H_2}$ and b are expected to be similar for anaerobic organisms regardless of the TEAP (Lovley and Goodwin 1988; Robinson and Tiedje 1984; Anderson et al. 2003), whereas both $K_S^{H_2}$ and $Y_{\frac{cell}{H_2}}$ are dependent upon the amount of energy available to the particular form of respiration (Lovley and Goodwin 1988; Robinson and Tiedje 1984; Anderson et al. 2003). The more energetically favorable the reaction the lower the $K_S^{H_2}$ and the higher the $Y_{\frac{cell}{H_2}}$ values. While Eqn. 2 does not predict the steady-state H_2 concentrations observed in the field (discussed below), it does predict the observed trends, where sediments with more energetically favorable forms of respiration have lower steady-state hydrogen concentrations than sediments in which the respiration is less favorable.

H_2 Monod Kinetics for Two-Phase (Aqueous/Gaseous) System. In a system containing both gaseous (headspace) and aqueous hydrogen, hydrogen consumption can be written using Monod kinetics in terms of the total moles of hydrogen (H_T) in the system, with biodegradation only occurring in the aqueous phase:

$$\frac{dH_T}{dt} = -\frac{\mu_{max}^{H_2}}{Y_{\frac{cell}{H_2}}} \frac{C_{H_2}}{K_S^{H_2} + C_{H_2}} XV_{aq} \tag{3}$$

where the total moles of hydrogen in the reactor are defined as

$$H_T = C_{H_2} V_{aq} + C_{H_2}^{hs} V_{hs} \tag{4}$$

and where $C_{H_2}^{hs}$ is the H_2 concentration in headspace (moles/L); V_{aq} is the liquid volume (L); and V_{hs} is the headspace volume (L). Eqn. 3 can be written in terms of the partial pressure of hydrogen in the headspace via the use of Otswalt's coefficient (Wilhelm et al. 1977; Löffler et al 1999), which assumes equilibrium partitioning of hydrogen between the aqueous and headspace phases. Using Otswalt's coefficient and the ideal gas law, we can write

$$C_{H_2} = \left(\frac{L}{RT} P_{H_2} \right) \tag{5}$$

and

$$C_{H_2}^{hs} = \left(\frac{P_{H_2}}{RT} \right) \tag{6}$$

where L is Otswalt's coefficient for hydrogen (0.01887 at 30ºC, Wilhelm et al. 1977); P_{H2} is the partial pressure of H_2 in headspace (atm); R is the universal gas constant $\left(0.0821 \frac{L \cdot atm}{K \cdot mole} \right)$; and T is the temperature (^oK). Substituting Eqn.'s 4 to 6 into Eqn. 3 results in the Monod equation written in terms of the partial pressure of hydrogen in the headspace.

$$\frac{dP_{H_2}}{dt} = -\frac{\mu_{max}^{H_2}}{\hat{Y}_{\frac{cell}{H_2}}} \frac{P_{H_2}}{\hat{K}_S^{H_2} + P_{H_2}} X \tag{7}$$

where the modified Monod parameters, written in terms of the partial pressure of hydrogen, are defined as

$$\hat{Y}_{\frac{cell}{H_2}} \equiv Y_{\frac{cell}{H_{H_2}}} \frac{V_{aq} L + V_{hs}}{V_{aq} RT} \tag{8}$$

$$\hat{K}_S^{H_2} \equiv K_S^{H_2} \frac{RT}{L} \tag{9}$$

The term $\hat{Y}_{\frac{cell}{H_2}}$ is the "observed" yield, which based solely on the measured hydrogen in the headspace (i.e., # cells produced per atm hydrogen removed from the headspace), while $Y_{\frac{cell}{H_2}}$ is the "true" yield based on the total moles of hydrogen utilized in the reactor (i.e., # cells produced per total moles of hydrogen consumed from entire reactor). In a similar manner, the Monod kinetics for biomass growth on hydrogen is given by

$$\frac{dX}{dt} = \mu_{max}^{H_2} \frac{P_{H_2}}{\hat{K}_S^{H_2} + P_{H_2}} X - bX \tag{10}$$

Dual-Electron Donor H_2 Kinetics. During a metal-radionuclide bioremediation scheme where an organic carbon source is injected into the subsurface, the simultaneous utilization of the carbon source and hydrogen is expected to affect the uptake kinetics of either substrate (Anderson and Lovley 2002; Lovley 1995). At this time, little is known regarding the simultaneous utilization of carbon and hydrogen and their interactions on bacterial growth. For this study, with acetate used as the organic carbon source, it was hypothesized that the simultaneous acetate and hydrogen utilization can be described using competitive inhibition kinetics. In addition, a saturation kinetic term was included for the electron acceptor (in this case Fe^{3+}) in the Monod expression. Written in terms of the hydrogen partial pressure, in a manner similar to the derivation of Eqn.'s 7 to 10, gives the following system of equations:

$$\frac{dP_{H_2}}{dt} = -\frac{u_{max}^{H_2}}{\hat{Y}_{\frac{cell}{H_2}}} \frac{P_{H_2}}{\hat{K}_S^{H_2} + P_{H_2} + \hat{K}_I^c C_c} \cdot \frac{C_{Fe^{3+}}}{K_{Fe^{3+}}^{H_2} + C_{Fe^{3+}}} X \tag{11}$$

$$\frac{dC_c}{dt} = -\frac{u_{max}^c}{Y_{\frac{cell}{c}}} \frac{C_c}{K_S^c + C_c + \hat{K}_I^{H_2} P_{H_2}} \cdot \frac{C_{Fe^{3+}}}{K_{Fe^{3+}}^c + C_{Fe^{3+}}} X \tag{12}$$

$$\frac{dC_{Fe^{3+}}}{dt} = \hat{Y}_{\frac{Fe^{3+}}{H_2}} \frac{dP_{H_2}}{dt} + Y_{\frac{Fe^{3+}}{c}} \frac{dC_c}{dt} \tag{13}$$

$$\frac{dX}{dt} = -\hat{Y}_{\frac{cell}{H_2}} \frac{dP_{H_2}}{dt} - Y_{\frac{cell}{c}} \frac{dC_c}{dt} - bX \tag{14}$$

where the modified Monod parameters, written in terms of the partial pressure of hydrogen, are defined as

$$\hat{Y}_{\frac{Fe^{3+}}{H_2}} \equiv Y_{\frac{Fe^{3+}}{H_2}} \frac{V_{aq} L + V_{hs}}{V_{aq} RT} \tag{15}$$

$$\hat{K}_I^c \equiv K_I^c \frac{RT}{L} \tag{16}$$

$$\hat{K}_I^{H_2} \equiv K_I^{H_2} \frac{L}{RT} \tag{17}$$

where C_C and $C_{Fe^{3+}}$ are the organic carbon and Fe^{3+} concentrations, respectively (moles/L); K_S^c is the half saturation constant for acetate (moles/L); $K_{Fe^{3+}}^{H_2}$ and $K_{Fe^{3+}}^c$ are the half saturation constants for iron reduction with hydrogen and acetate as the electron

donors, respectively (moles/L); μ^{c}_{max} is the maximum specific growth rate on acetate (time^{-1}); $K_I^{H_2}$ (moles/L-atm) and K_I^{c} (atm-L/mole) are the competitive inhibition constants for hydrogen and acetate, respectively; $Y_{\frac{cell}{c}}$ is the bacterial cell yield coefficient (# cells /mole acetate); and $Y_{\frac{Fe^{3+}}{H_2}}$ and $Y_{\frac{Fe^{3+}}{c}}$ are the yield coefficients, moles of iron(III) consumed per mole of hydrogen or acetate utilized, respectively (mole/mole). An advantage of the proposed multi-substrate utilization expressions is that the steady-state hydrogen concentrations representative for different TEAPs can be estimated from the knowledge of the degradation kinetics of the hydrogen source and the carbon source. This is accomplished similar to the derivation of Eqn. 2 by setting Eqn. 14 to zero and solving for the hydrogen concentration.

Parameter Estimation. Parameter estimation was carried out by developing a C-computer code based on Eqn.'s 11 to 14 and linking it to the model-independent nonlinear parameter estimation code PEST (Version 6.05, Watermark Numerical Computing). For this study, PEST was used to determine one set of Monod parameters that optimally fit multiple experimental runs simultaneously. For example, results from multiple sole-electron donor experiments with acetate at varying initial concentrations were used simultaneously to develop one set of Monod parameters that optimally fit all the experimental results. Parameter estimations were carried out this way to determine Monod parameters for acetate and H_2 as sole electron donors. For this analysis cell decay was neglected because of the short experimental durations (Lui et al. 2002). The sole-donor Monod parameters were then applied to the dual-donor experimental results, and PEST was used to determine one set of inhibition coefficients simultaneously for all dual-donor experiments.

Results and Discussion

Batch experiments quantified the growth of *G. sulfurreducens* in test tubes containing a bicarbonate buffered ferric citrate solution amended with trace vitamins and minerals and supplied either actetate, H_2, or combination of the two as the electron donor. The test tubes were incubated at 30˚C and separate test tubes were destructively analyzed for Fe^{2+}, acetate, hydrogen and cell numbers at each time point. All test tubes inoculated with hydrogen were incubated on their side to maximize hydrogen diffusion from the headspace into solution. Three single-electron donor experiments were conducted with acetate as the electron donor at aqueous concentrations ranging from 0.74 mM to 8.6 mM. Five single-donor experiments were conducted with hydrogen as the electron donor at initial headspace partial pressures ranging from ~10^{-5} atm to ~10^{-2} atm (aqueous concentrations ranging from ~0.01 μM to ~6 μM). In addition, three dual-donor experiments were conducted with both acetate and hydrogen available as electron donors.

Results from the single donor experiments showed simultaneous depletion of electron donor (acetate or hydrogen) and Fe^{3+}, and growth of biomass during suspended growth experiments (Figure 1) while control samples showed no abiotic loss of H_2 or acetate, or production of Fe^{2+}, during the course of the experiments (data not shown). It

was found during the biodegradation experiments that there was a constant lag period of approximately 21 hours during all of the acetate biodegradation experiments. A lag period was also observed for the hydrogen experiments. However, the lag period varied between experiments, ranging from no lag period to approximately 12 hours. The observed lag periods for acetate and hydrogen were accounted for in the numerical model by delaying the start of the biodegradation until the end of the experimentally-observed lag time, and the Monod parameters (Table 1) were determined as described above.

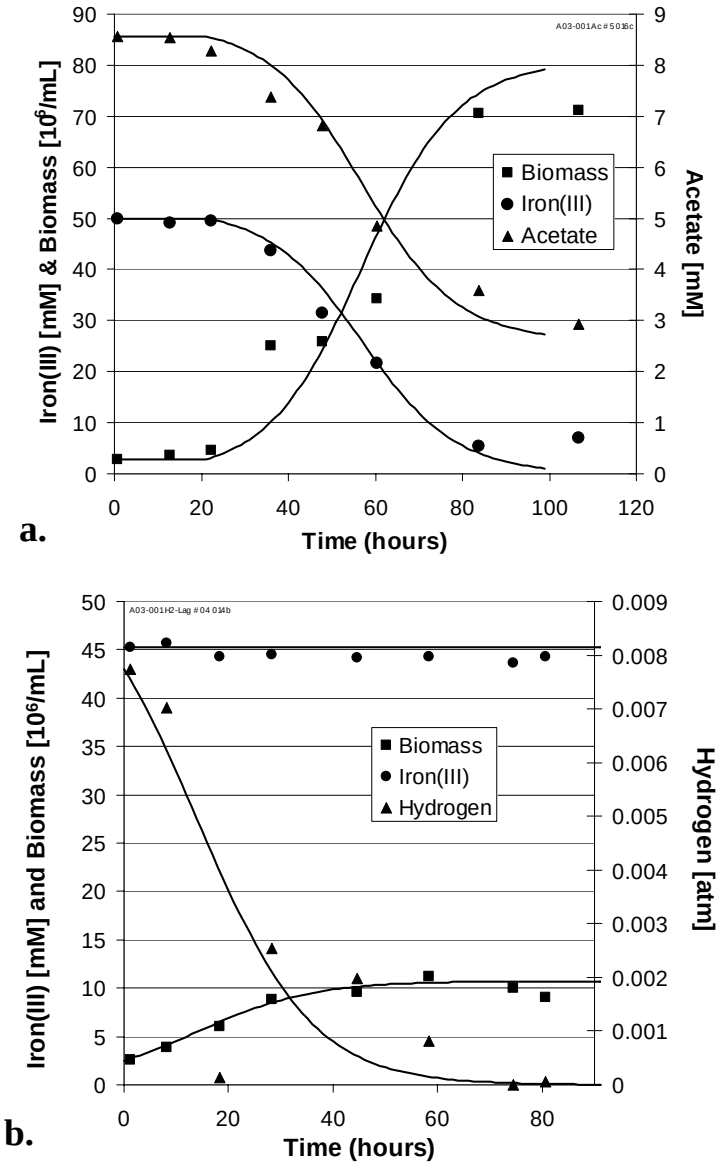

Figure 1 Representative results for a) acetate and b) H_2 consumption under Fe^{3+} reducing conditions. Symbols are experimental results. Lines are model results using parameters in Table 1.

It was found during the parameter estimation process for hydrogen consumption that $\mu_{max}^{H_2}$ and $\hat{K}_S^{H_2}$ were very well correlated (correlation coefficient > 0.999), indicating that $\hat{K}_S^{H_2} > P_{H_2}$. Our starting aqueous hydrogen concentrations were ≤ 6 μM, and while half-saturation constants for hydrogen utilization under iron-reducing conditions are not readily available in the literature, reported values for hydrogen utilization by sulfate reducing and methanogenic organisms are in this range (Robinson and Tiedje 1984; Ahring et al. 1991) and support the results indicating that $\hat{K}_S^{H_2} > P_{H_2}$. In addition, as shown in Figure 1b, Fe^{3+} depletion was minimal during the hydrogen biodegradation experiments, and as such, Monod parameters for Fe^{3+} could not be determined from the hydrogen data sets. During the acetate parameter estimation, it was found that μ_{max}^{c} and $K_{Fe^{3+}}^{c}$ were also very well correlated (correlation coefficient > 0.999), indicating that $K_{Fe^{3+}}^{c} > C_{Fe^{3+}}$. With these correlations, Eqn.'s 11 and 12 can be rewritten as follows, where the terms in brackets are considered as one parameter:

$$\frac{dP_{H_2}}{dt} = -\frac{1}{\hat{Y}_{\frac{cell}{H_2}}}\left[\frac{u_{max}^{H_2}}{\hat{K}_S^{H_2}}\right]\frac{P_{H_2}}{1+\left[\frac{\hat{K}_I^{c}}{\hat{K}_S^{H_2}}\right]C_c}X \tag{18}$$

$$\frac{dC_c}{dt} = -\frac{1}{Y_{\frac{cell}{c}}}\left[\frac{u_{max}^{c}}{K_{Fe^{3+}}^{c}}\right]\frac{C_c C_{Fe^{3+}}}{K_S^{c} + C_c + \hat{K}_I^{H_2}P_{H_2}}\cdot X \tag{19}$$

In the dual-donor batch experiments, *G. sulfurreducens* utilized acetate and H_2 simultaneously with ferric citrate as the electron acceptor (Figure 2). To determine the effect of the presence of one donor on the utilization of the other, the single-donor kinetic parameters for iron reduction with either H_2 or acetate as the electron donor were used in dual-donor model simulations with and without competitive inhibition. The inhibition parameters $\left(K_I^{H_2} \text{ and } \frac{K_I^{c}}{K_S^{H_2}}\right)$ were estimated simultaneously by PEST and the parameters are shown in Table 1. Figure 2 show the experimental data along with the model results with and without inhibition (i.e., $K_I^{H_2} = K_I^{c} = 0$) for a representative dual-electron donor experiment. Analysis of the weighted-least-squares residuals between the experimental data and the model results showed that there is a minor decrease in residuals when including the inhibition terms. Residuals for acetate, hydrogen, and iron were reduced, with the largest contribution being from iron, while those for biomass increased. This suggests that slight inhibition is occurring between hydrogen and acetate under the conditions of these experiments. To our knowledge, this study was the first to compare the impact of acetate and hydrogen on the kinetics of each other during iron reduction.

Table 1. Kinetic parameters of *G. sulfurreducens* during iron reduction with acetate and/or hydrogen as the electron donor. Parameters are specified for aqueous hydrogen concentrations. Parameters in terms of headspace hydrogen can be calculated with Eqn.'s 8, 9, 15-17. All parameters except $\frac{K_I^c}{K_S^{H_2}}$ and $K_I^{H_2}$ were obtained from single-donor experiments.

Acetate		Hydrogen	
Parameter	**Value**	**Parameter**	**Value**
$\frac{\mu_{max}^c}{K_{Fe^{3+}}^c}$	0.00184 $(hr\text{-}mM)^{-1}$	$\frac{\mu_{max}^{H_2}}{K_S^{H_2}}$	12.2 $(hr\text{-}mM)^{-1}$
$Y_{\frac{cell}{c}}$	11.03 $\frac{10^9 \text{ cells}}{\text{mmole Acetate}}$	$Y_{\frac{cell}{H_2}}$	16.3 $\frac{10^9 \text{ cells}}{\text{mmole} H_2}$
K_S^c	0.124 mM	$K_{Fe^{3+}}^{H_2}$	ND
$Y_{\frac{Fe^{3+}}{c}}$	8.39 $\frac{\text{mM} Fe^{3+}}{\text{mM Acetate}}$	$Y_{\frac{Fe^{3+}}{H_2}}$	ND
$\frac{K_I^c}{K_S^{H_2}}$	0.271 mM^{-1}	$K_I^{H_2}$	959 $\frac{mM}{mM}$

ND = Not determinable

Comparison of the kinetic parameters for H_2 utilization under iron reducing conditions from this study to kinetic parameters previously determined for hydrogen utilization under methanogenic and sulfate-reducing conditions (Lovley and Goodwin 1988) did show that the more energetically favorable the reaction, the lower the half saturation constant and the higher the cell yield (Table 2). However, model analysis utilizing only the physiological parameters of the hydrogen-consuming microorganisms did not correlate with steady-state H_2 values measured by researchers in the field (Chapelle et al. 1996; Chapelle et al. 2002; Lovley et al.1994) (Table 2). An obvious explanation for this discrepancy is that the kinetic coefficients measured in the laboratory under ideal growth conditions differ from those in the field. In addition, it is possible that in the field there are mechanisms driving the steady-state hydrogen concentrations down from those predicted assuming hydrogen is the sole growth substrate. One possible mechanism is the interaction of H_2 with additional electron donors. Hydrogen is usually not the sole electron donor present where field observations of H_2 concentrations have been correlated to TEAPs. Other electron donors include petroleum hydrocarbons in contaminated aquifers (Chapelle et al. 1995; Chapelle et al. 2002; Vroblesky et al. 1996) or natural organic matter in pristine aquifers (Chapelle et al. 1995). In addition, fermentation of organic matter is not only a source of H_2, but also of additional

fermentation products, such as acetate, which can serve as electron donors for TEAPs. Limiting concentration of electron acceptor is another possible mechanism that can influence the steady-state H_2 concentration.

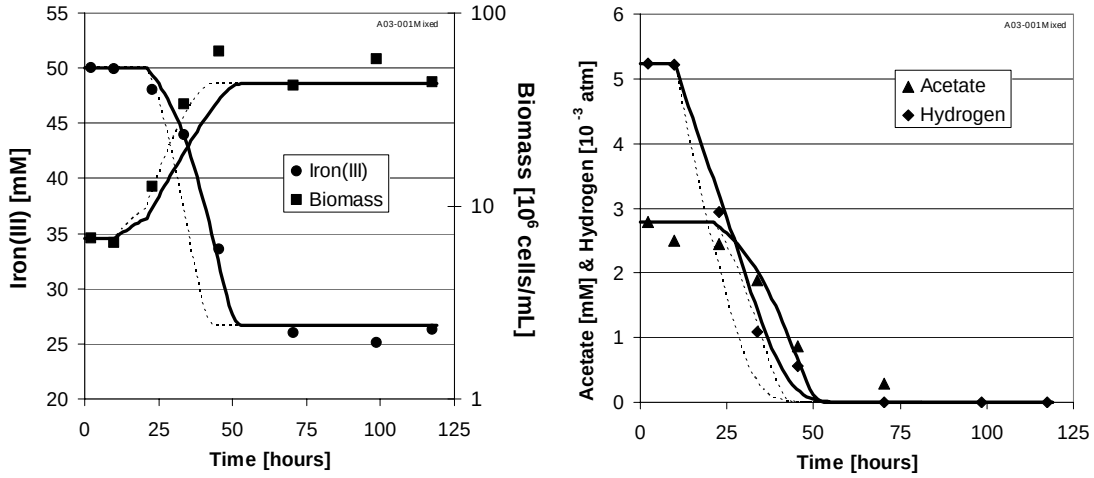

Figure 2. Dual-electron donor experiments with simultaneous utilization of acetate and hydrogen. Solid symbols are experimental results. Lines are model results using parameters in Table 1 with inhibition (solid) and without inhibition (dashed). Initial conditions are 3mM Acetate & 0.005 atm H_2.

Further model analysis showed that there is a unique steady-state H_2 concentration that occurs for acetate concentrations below the half saturation constant, independent of the Fe(III) concentration and of whether there is any inhibition occurring between the acetate and hydrogen (Figure 3). While the steady-state H_2 concentrations predicted using the laboratory-derived coefficients from this study (30 ^oC, and ferric citrate as Fe(III) source) are higher than those observed in the field (usually closer to 15 ^oC and solid phase Fe(III)), this does provides a possible explanation why there are consistent ranges of H_2 concentrations in the field for a given TEAP. For field conditions, there must be a balance between H_2 and other electron donors present, and the terminal electron acceptor if it is limiting, for steady-state hydrogen concentrations to be achieved. In the subsurface, this balance is a complicated function of the rate-limited availability of these compounds. For example, H_2 availability is related to the fermentation rate of organic substrates, and the organic substrate availability may be rate limited, such as dissolution from a NAPL. Furthermore, the iron source used in these experiments was soluble ferric citrate. In aquifer sediments, Fe^{3+} availability may be rate-limited due to microbially-mediated dissolution from more insoluble Fe^{3+} oxides. From a numerical modeling standpoint, these rates would affect the steady-state hydrogen concentration.

Table 2. Potential energy of reaction, cell yield coefficient, first-order growth rates, as well as measured and calculated H_2 levels for different terminal electron acceptor processes with hydrogen as the sole electron donor.

TEAP	$\Delta G^{o'}$ (kJ/ mole H_2)	$Y_{\frac{cell}{H_2}}$ (g protein/ mole H_2)	$\left[\frac{\mu_{max}^{H_2}}{K_S^{H_2}}\right]^{(c)}$ or $\left[\frac{V_{max}^{H_2} Y}{K_m^{H_2}}\right]^{(b)}$ $(hr\text{-}\mu M)^{-1}$	H_2 Field Data[e]	H_2 as sole electron donor [f]
Methanogenesis	-34 [a]	0.20 [b]	3.22×10^{-4} [b]	5-30 nM	1305 nM
Sulfate Reduction	-38 [a]	0.85 [b]	4.68×10^{-3} [b]	1-4 nM	90 nM
Iron Reduction	-228 [a]	2.5 [c,d]	1.20×10^{-2} [c]	0.2-0.8 nM	52 nM

(a) Löffler et al. 1999. $\Delta G^{o'}$ for iron reduction is for soluble Fe(III).
(b) Robinson and Tiedje 1984. Used Michaelis-Menton coefficients from this manuscript, as the authors considered their Monod coefficients to be general estimates. $V_{max}^{H_2}$ = 0.11 μmol/min/mg for both methanogens and sulfate-reducers and K_m = 4.1 μM for methanogens and 1.2 μM for sulfate-reducers. Note that the yield coefficients given in Table 3 of this reference are a typographical error. The correct values are presented above.
(c) This research
(d) 1 cell = 2.8×10^{-13}g and 1g cell = 0.55 g protein (for *E. coli* cell) (Madigan et al. 1997)
(e) Chapelle et al. 1997
(f) Calculated from Eqn. 2.

Conclusion

This research and subsequent modeling analysis showed that the presence of a carbon source had a slight effect on steady-state H_2 levels, but that for low carbon concentrations ($<< K_S^c$) H_2 levels remain rather stable. Given the consistent H_2 levels found in groundwaters for a specific TEAP under a wide variety of conditions, this indicates that these H_2 levels in the field are rather robust, and suggests that steady-state H_2 levels observed in aquifers cannot be predicted based on kinetic coefficients measured under ideal growth conditions in laboratory settings. The inability of the current dataset to provide an accurate estimate of the K_s for H_2 uptake by *G. sulfurreducens* does not jeopardize this conclusion, since the available data suggest, as in the case of pure cultures of sulfate-reducing and methanogenic microorganisms, that the half saturation constant for H_2 uptake by this organism under ideal growth conditions in the laboratory is likely to be in the μM rather than the nM range.

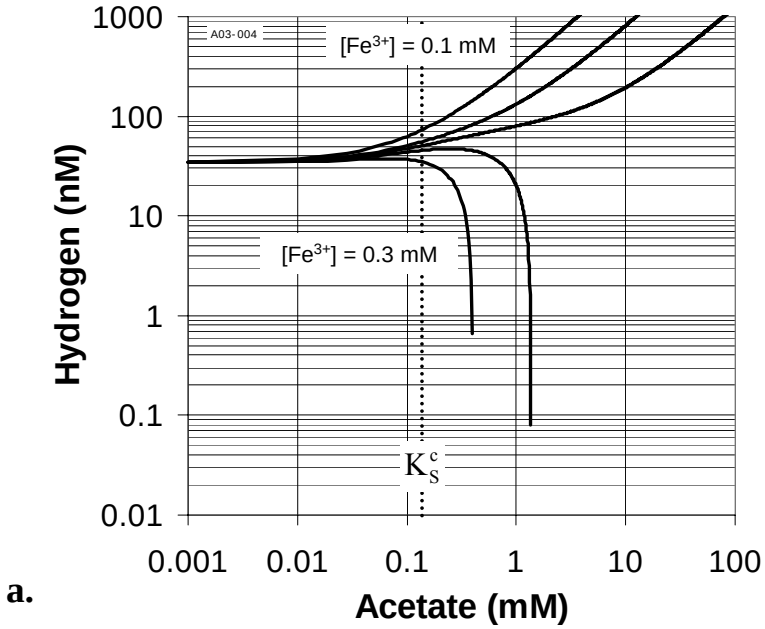

a.

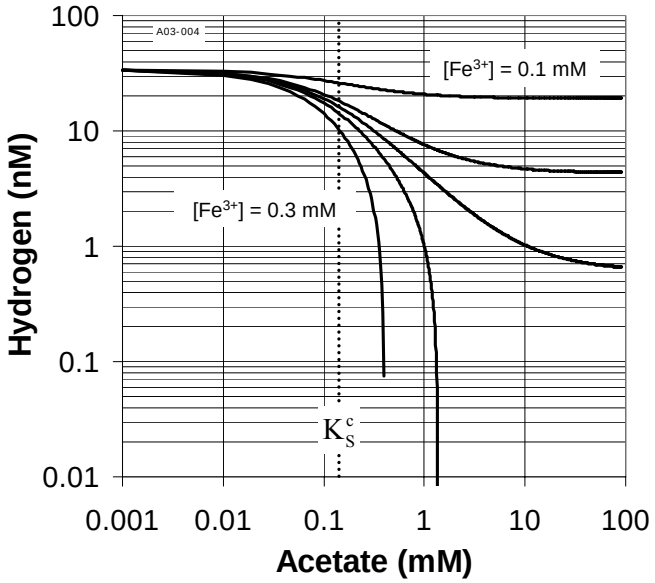

b.

Figure 3. Steady-state aqueous hydrogen concentration as a function of acetate and Fe^{3+}. Fe^{3+} concentrations are 0.3, 0.25, 0.225, 0.2, and 0.1 mM. Curves calculated from Eqn. 14 using coefficients in Table 1. Figure (a) is with no inhibition between electron donors, and figure (b) uses inhibition coefficients in Table 1. Dashed line is the Monod half-saturation constant for acetate degradation (Table 1).

2. Effect of Iron Bioavailability on Dissolved Hydrogen Concentrations during Microbial Iron Reduction

Introduction

During a biostimulation scenario in which a carbon source is added into the subsurface to facilitate the reduction and precipitation of uranium, it is important to monitor which terminal electron accepting process (TEAP) is occurring at a particular time and space in order to understand and maximize the biotransformation process. Dissolved H_2 has been shown to be an indicator of TEAPs in the subsurface (Chapelle et al. 1996; Chapelle et al. 2002; Lovley et al.1994) with specific H_2 concentration ranges measured for different TEAPs; nitrate reduction (<0.1 nM), iron reduction (0.2-0.8 nM), sulfate reduction (1-4 nM), methanogenesis (5-15 nM). The TEAP yielding the most energy (if that electron acceptor is present) proceeds before the TEAPs yielding less energy because the microbial population for the higher energy-yielding TEAP is able to utilize the H_2 more efficiently, thus driving the H_2 concentration to levels that cannot be utilized by lower energy-yielding TEAPs (Lovley & Goodwin 1988). For example, the presence of sulfate (> 6-9 mg/l) has been shown to inhibit methanogenesis (Chapelle et al. 1995) and the presence of amorphous Fe(III) has been documented to inhibit both sulfate reduction and methanogenesis (Lovley & Phillips 1987). Contrary to this, research has shown that iron reduction can occur simultaneously with sulfate reduction (Watson et al. 2003) even though more energy is gained from iron reduction. One possible explanation for both processes to occur simultaneously is that the limited availability of the iron to the iron reducing microorganisms (referred throughout as "bioavailability") decreases the potential rate of iron reduction, and even though iron is present, it cannot be reduced fast enough to outcompete lower energy yielding TEAPs. Electron shuttling compounds such as AQDS (9,10-anthraquinone-2,6-disulfonic acid) have been shown to increase iron bioavailability in soil (Hacherl et al. 2001; Lovley et al. 1996; Nevin & Lovley 2000) by acting as an electron shuttle between iron surfaces and iron reducing microorganisms that are not in direct contact with the surface bound iron, which significantly increases the rate of iron reduction in soils.

It is unknown to what degree changes in iron bioavailability will affect steady-state H_2 levels during iron reduction. Iron bioavailability may change 1) as the more bioavailable fraction of iron is being reduced and less available iron remains, 2) as Fe(II) sorbs onto the Fe(III) phase, which may block Fe(III) reaction sites, and 3) as the bioavailability of iron is increased in the presence of AQDS or other electron shuttling compounds. The objective of this study was to determine via flow-through column experiments how changes in iron bioavailability during long-term iron reduction and/or due to the addition of AQDS affect iron reduction rates and subsequent steady-state H_2 levels. The results of this research will increase existing knowledge pertaining to the use of H_2 as an indicator of redox processes, specifically iron reduction, during bioremediation.

Results and Discussion

A 30 cm long x 5 cm diameter flow-through column with sampling ports every 2 cm along the length of the column was filled with previously unsaturated background Field Research Center (FRC) soil and supplied a phosphate buffered media amended with 3 mM acetate to monitor iron reduction over time by indigenous microorganisms in a simulated biostimulation scenario. Iron reduction was first detected after 32 days of acetate addition and continued until between 200-300 days (Figure 4) when the Fe(II) concentration leveled off at 37.3 ± 7.8 µmol/g dry soil (n=13). An iron reduction rate of 0.17 µmol/g soil-d was calculated using linear regression of Fe(II) production over time. No Fe(II) was measured in the pore water of the column throughout the experiment indicating that the majority of the Fe(II) produced was sorbed to the soil. Uniform accumulation of Fe(II) at each sampling point over time indicated similar rates of iron reduction throughout the column and coincided with a change in the soil color from a brown/orange color to a gray color.

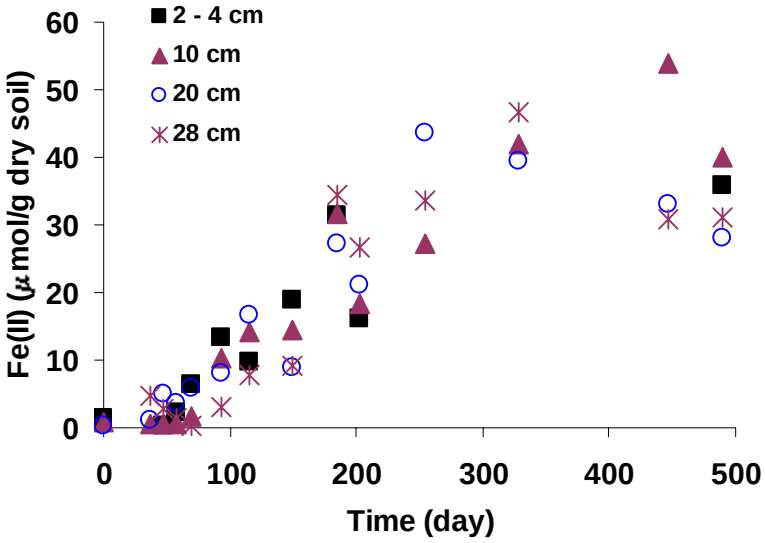

Figure 4. Fe(II) concentrations over time at different sampling points along the length of the 30 cm column filled with FRC soil. Samples were extracted for 1hr in 0.5 N HCl.

After 497 days of operation, the column was destructively sampled and the Fe(II) and total extracted iron concentration profile along the length of the column was measured. The iron concentrations were relatively constant along the length of the column with measured Fe(II) and total extracted iron concentrations of 38.6 ± 8.6 µmol/g dry soil (n=12) and 36.1 ± 7.4 µmol/g dry soil (n=12), respectively, after 1 hour extraction in 0.5 N HCl. The Fe(II) and total extracted iron concentrations measured after the column was destructively sampled agree well with the steady-state sorbed Fe(II) and total extracted iron concentrations. Increased Fe(II) concentrations were measured with increased extraction time between extraction times of 1 hour, 22 hours and 21 days, with the majority of the Fe(II) (77.2 %) measured after 22 hours of extraction. Therefore,

quantification of Fe(II) using only 1 hour of extraction time in 0.5N HCl would have significantly underestimated the total amount of Fe(II) produced after 500 days of iron reduction.

Within the first five days of acetate addition to the column, H_2 levels decreased below 0.3 nM before starting to increase after day 36 and leveling off after approximately 90 days. Throughout the duration of the experiment, steady-state H_2 concentrations fluctuated between 0.3 nM and 25 nM with an average H_2 concentration between day 92 and day 422 of 3.9 nM (Figure 5). Steady-state acetate concentrations (day 36 to day 453) decreased from 3.0 mM at the beginning of the column to 2.5 mM at the effluent (*p-value* < 0.001) with the majority of the acetate degradation occurring between the influent sampling port (just upstream of the acetate addition point) and the first sampling port (2 cm into the column).

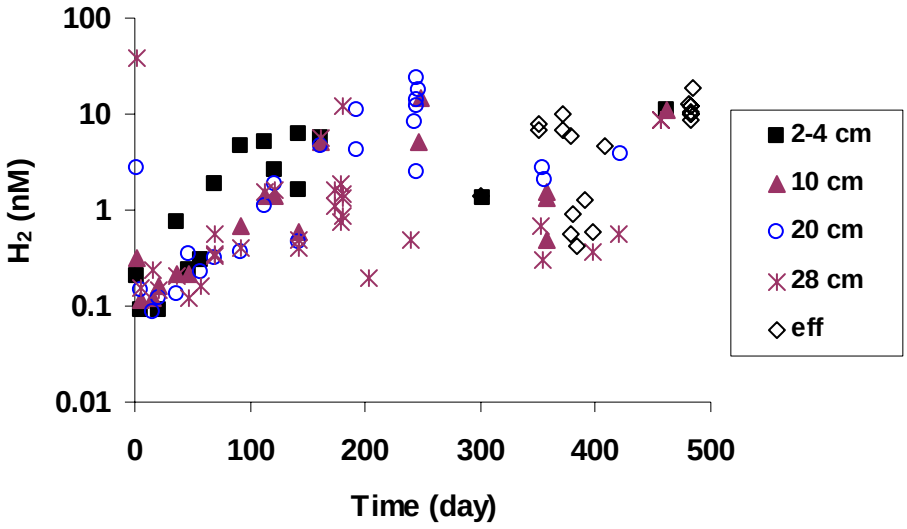

Figure 5. Dissolved hydrogen concentrations over time at different sampling points along the length of the 30 cm column filled with FRC soil.

Sulfate was present in the influent media as part of the trace mineral solution at a concentration of 0.28 mM (27 mg/l). Sulfate concentrations were first measured in the column after 100 days of column operation with sulfate reduction first observed on day 208. Between day 208 and day 466, steady-state sulfate concentrations decreased from 0.28 mM at the influent to 0.24 mM at the effluent (*p-value* < 0.001). Similar to the fate of acetate in the column, the majority of the sulfate removal occurred before the first sampling port of the column. In addition, qualitative evidence of sulfate reduction was observed through the presence of sulfide odor and the formation of a black precipitate throughout the column. Sulfate concentrations throughout the experiment ranged from 15 to 30 mg/L, which is above the minimum sulfate concentration reported to inhibit methanogenesis in aquifers (4 to 6 mg/l) (Chapelle et al. 1995; Chapelle et al. 2002). Methane was not detected throughout the column when analyzed for on day 146. Therefore iron reduction appears to have been the dominant terminal electron accepting

process (TEAP) in this system throughout the duration of the experiment, though the average H_2 concentration (3.9 nM) was higher than reported in the literature for iron reducing zones (0.2 nM – 0.8 nM) (Chapelle et al. 1996; Chapelle et al. 2002; Lovley et al. 1994).

Simultaneous iron and sulfate reduction has also been measured in a long-term batch experiment using aquifer sediments (Watson et al. 2003) in which H_2 concentrations during iron reduction were not always in the range typically reported for iron reducing conditions. Though amorphous iron has been shown to inhibit sulfate reduction and methanogenesis (Lovley & Phillips 1987), significant increases in spatial and temporal Fe(II) concentrations are measured in aquifers where other TEAPs that are less energetically favorable (sulfate reduction, methanogenesis) are active and considered to be the dominant TEAP due to higher H_2 concentrations (Lovley et al. 1994; Chapelle et al. 1995; Chapelle et al. 1996; Chapelle et al. 1997). One possible reason for less energetically favorable TEAPs occurring in iron reducing zones is that, due to the less bioavailable fraction present in aquifer sediments, the bioavailability of Fe(III) limits competitive exclusion of H_2 concentrations. In an attempt to increase iron bioavailability, AQDS was added as part of the 3 mM acetate feed media supplied to a 1 cm diameter, 15 cm long column filled with FRC soil and inoculated with *Geobacter sulfurreducens* while a parallel control column was not supplied AQDS. Enhancement of iron bioavailability through AQDS addition not only increased the rate of iron reduction from 0.16 μmol (g soil)$^{-1}$day^{-1} to 0.35 μmol (g soil)$^{-1}$day^{-1}, but also decreased steady-state H_2 concentrations (Figure 6) from 4.0 nM (± 3.1 nM, n=23) to 2.0 nM (± 1.2 nM, n=29), which was a statistically significant decrease ($p < 0.005$, n=23). In addition, less variability in H_2 concentrations over time was measured in the column supplied with AQDS. Steady state H_2 concentrations in the column supplied with AQDS, though lower than the column without AQDS, were still higher than reported in the literature for iron reducing conditions (0.2 nM – 0.8 nM) (Chapelle et al. 1996; Chapelle et al. 2002; Lovley et al. 1994). It is important to note that all column experiments were performed at 30ºC, which is significantly higher than field conditions (15ºC or less, for which H_2 levels are reported) and supplied a variety of trace vitamins and minerals that may be limiting in an aquifer and which would affect the biokinetic coefficients. Hoehler et al. (1998) demonstrated that a decrease in temperature from 30ºC to 15ºC decreased H_2 concentrations in batch experiments by a factor of 5.0 and 5.4 for sulfate reducing and methanogenic conditions, respectively. Applying this temperature dependency to the H_2 concentrations reported here decreases the steady-state H_2 concentrations for all column experiments in this study to within the range reported for iron-reducing conditions in the field. Model analysis using biokinetic coefficients obtained from more ideal growth conditions (soluble Fe(III), 30º C, trace vitamins and minerals addition) also predicted higher steady-state H_2 values compared to field data under iron reducing conditions (Brown et al. 2004).

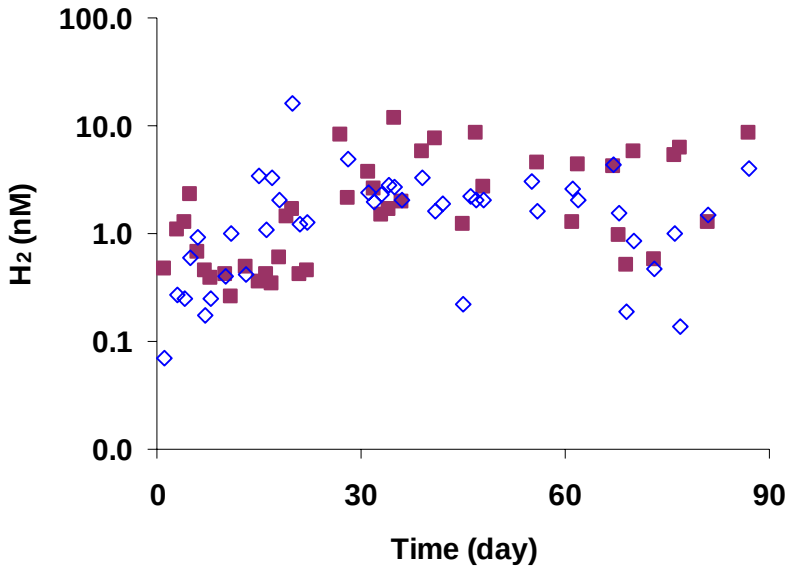

Figure 6. Dissolved H_2 concentrations over time from the effluent of flow-through column experiments without (square) and with (diamond) 50 µM AQDS addition.

The use of H_2 as an indicator of TEAPs assumes that the availability of the electron donor(s) is limiting. Electron donor limiting conditions would result in competition between different TEAPs with the more energetically favorable TEAP having an advantage over less energetically favorable TEAPs. However, research has shown that when the electron donor becomes less limiting, more than one TEAP can occur simultaneously (Vroblesky et al. 1996). This is a possible explanation as to why both iron and sulfate reduction occurred simultaneously in the long-term column experiment. Sulfate concentrations did decrease modestly, but statistically, along the length of the column suggesting that a small part of the electron flow went to sulfate, which would be expected if the electron donor limitation was not severe. The assumption that the electron donor was not limiting appears valid because only a small amount (0.5 mM) of the 3 mM influent acetate was consumed throughout the column.

Conclusion

Steady-state H_2 concentrations were similar between the long-term (500 day) column experiment utilizing only the indigenous iron-reducing populations and the short-term column experiment that was supplemented with *G. sulfurreducens*, though the column supplied *G. sulfurreducens* reached steady-state conditions significantly faster. In addition, more Fe(II) was produced in columns with *G. sulfurreducens* when destructively sampled after 96 days compared to the Fe(II) concentration in the long-term column without *G. sulfurreducens* at the same time point. Though the column inoculated with *G. sulfurreducens* (but not supplied AQDS) reached steady-state conditions faster than the column not supplied *G. sulfurreducens*, the rate of iron reduction calculated in the column with *G. sulfurreducens* (0.16 µmol (g soil)$^{-1}$day^{-1}) was similar to the rate of iron reduction calculated for the column without *G. sulfurreducens* (0.17 µmol (g soil)$^{-}$

$^{1}day^{-1}$). The addition of AQDS increased the rate of iron reduction from 0.16 μmol (g soil)$^{-1}day^{-1}$ to 0.35 μmol (g soil)$^{-1}day^{-1}$ and decreased the steady-state H_2 levels from 4.0 nM to 2.0 nM. H_2 concentrations have been shown to be solely dependent upon the physiological parameters of the hydrogen-consuming microorganisms (Lovley and Goodwin 1988) with the steady-state H_2 concentration inversely proportional to the rate of H_2 consumption. Accordingly, a doubling of the iron reduction rate through the addition of AQDS deceased the steady-state H_2 concentration by half. The long-term column experiment showed that a steady-state H_2 level was achieved when the Fe(II) production rate was constant, indicating that, as expected, pseudo-steady state conditions had been reached. The results of this study have shown that although steady-state H_2 levels during iron reduction are not unique and depend on factors such as the iron bioavailability, they remain relatively constant for particular conditions over extended time periods, and may be used to monitor changes in iron reduction rates. It should be cautioned that though average H_2 values compared well for different rates of iron reduction, H_2 levels fluctuated within a substantial range over time as measured in these small columns allowing only small sample sizes and low flow rates.

3. Influence Co-Electron Donor Concentration and Iron Bioavailability on Hydrogen as an Indicator of Redox Conditions

Model analysis from phase 1 of this research suggest that a carbon source added as an electron donor during a biostimulation scenario may influence the steady-state H_2 concentration for each terminal electron accepting process (TEAP) concentrations when the carbon concentration is above the carbon half saturation constant, K_S^C. To explore this possible correlation, a series of batch experiments were performed to quantify the kinetics of acetate utilization during the reduction of surface bound iron (iron oxide coated sand) by *Geobacter sulfurreducens*. These kinetics will be compared to batch iron reduction kinetics obtained using ferric citrate, a soluble form of Fe(III). This will follow with a series of column experiments using either ferric citrate or iron oxide coated sand (IOCS) as the electron acceptor to measure steady-state H_2 levels for acetate concentrations above, at, and below K_S^C. In addition, the effect of surface-bound iron availability to the iron-reducing organisms (or "bioavailability") was examined through the use of the electron shuttle compound, AQDS (9,10-anthraquinone-2,6-disulfonic acid).

The first set of batch experiments quantified the effect of AQDS on either soluble Fe(III) (ferric citrate) or surface bound iron (IOCS) reduction in test tubes inoculated with *Geobacter sulfurreducens* and supplied 0.7 mM acetate. The initial Fe(III) concentration in test tubes with ferric citrate or IOCS was 50 mM and 25 mM, respectively. The addition of AQDS did not affect the rate of soluble Fe(III) (ferric citrate) reduction (Figure 7) but the addition of AQDS did affect the rate of surface bound microbial Fe(III) reduction (Figure 8a) and acetate oxidation (Figure 8b). The amount of Fe(II) produced in the batch experiments supplied 0.7 mM acetate without and with AQDS was 3.8 mM and 4.3 mM, respectively. H_2 concentrations were also monitored over time in the IOCS batch experiments with and without AQDS (Figure 9) and show

that test tubes without AQDS had higher H_2 concentrations during iron reduction. This trend corresponds to the results of the column experiments using FRC soil with and without AQDS (Figure 6). Active iron reduction in the batch experiments due to acetate oxidation occurred until approximately 210 hours and 70 hours for the experiments without and with AQDS, respectively (Figure 8).

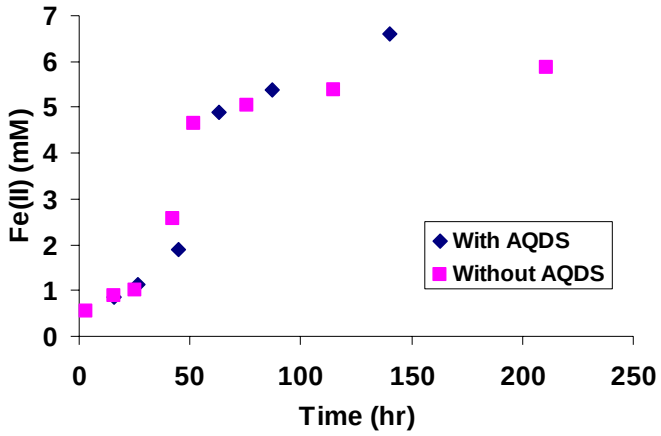

Figure 7. Effect of 50 μM AQDS on soluble iron reduction. Test tubes contained 50mM ferric citrate, 0.7mM acetate and were inoculated with *G. sulfurreducens*.

For both experiments, H_2 levels increase for the first half of the iron reduction zone and then decrease. *G. sulfurreducens* can utilize acetate and H_2 simultaneously. The rise in H_2 concentrations for the first 50 hours of the experiment may be due to *G. sulfurreducens* preferentially utilizing acetate at the beginning of the experiment even though the *G. sulfurreducens* culture inoculated into all test tubes at the beginning of all experiments was grown on H_2. The increase in H_2 concentrations during iron reduction may also be due to inhibition from acetate when acetate concentrations are above K_S^C. K_S^C for acetate was measured to be 0.125 mM during ferric citrate reduction (Table 1). Alternately, H_2 may be an intermediate of acetate degradation, which would explain the increase in H_2 at the beginning of each batch experiment. More information is needed with regard to the pathway(s) involved in H_2 and acetate degradation. Additional batch experiments are currently being performed that measure iron reduction using IOCS for starting acetate concentrations at and below the K_S^C previously measured during ferric citrate reduction to explore the link between H_2 and acetate concentrations during surface bound iron reduction.

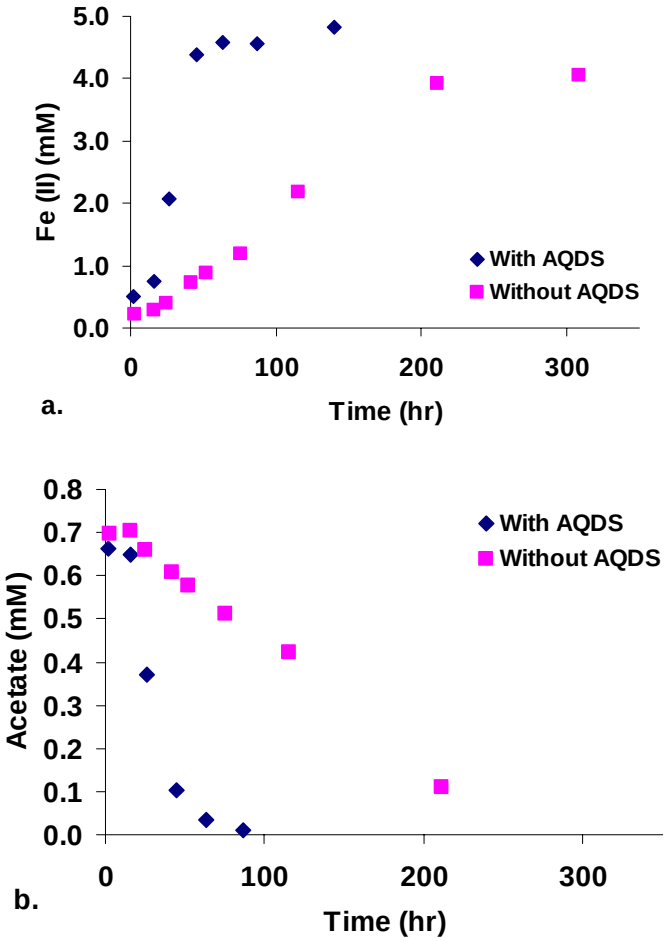

Figure 8. Effect of 50 μM AQDS on surface bound iron reduction. Test tubes contained 50 mM ferric citrate, 0.7 mM acetate and were inoculated with *G. sulfurreducens*. a) Fe(II) production. b) acetate utilization.

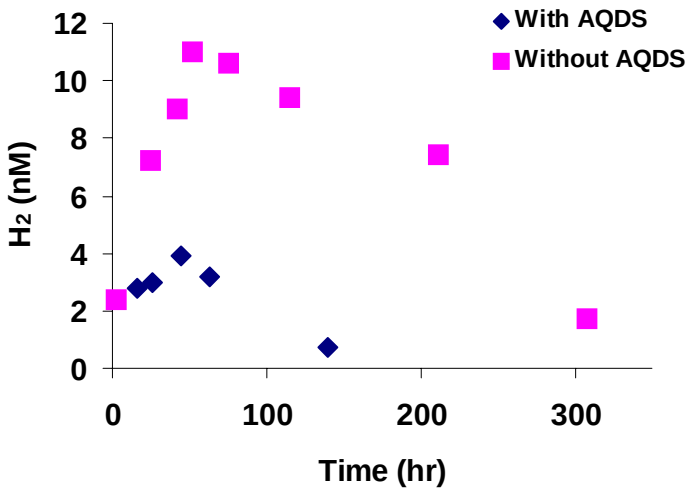

Figure 9. H_2 concentrations over time for surface bound iron reduction batch experiments with and without AQDS.

To measure steady-state H_2 concentrations during the reduction of a soluble Fe(III) source, a 30 cm long, 5 cm diameter column was filled with 1mm glass beads, inoculated with *G. sulfurreducens* and supplied 5 mM ferric citrate and 0.3mM acetate at a rate of 0.5ml/min. The column was fixed with sampling ports every two cm along the length of the column. After two days of column operation, acetate concentrations were below detection throughout the column. The profile of Fe(II) concentrations with time throughout the column indicate a sharp initial rise in Fe(II) production just after the start of the experiment which was followed by a slow increase in Fe(II) concentrations with time throughout the column with steady-state conditions occurring after approximately 40 days (Figure 10).

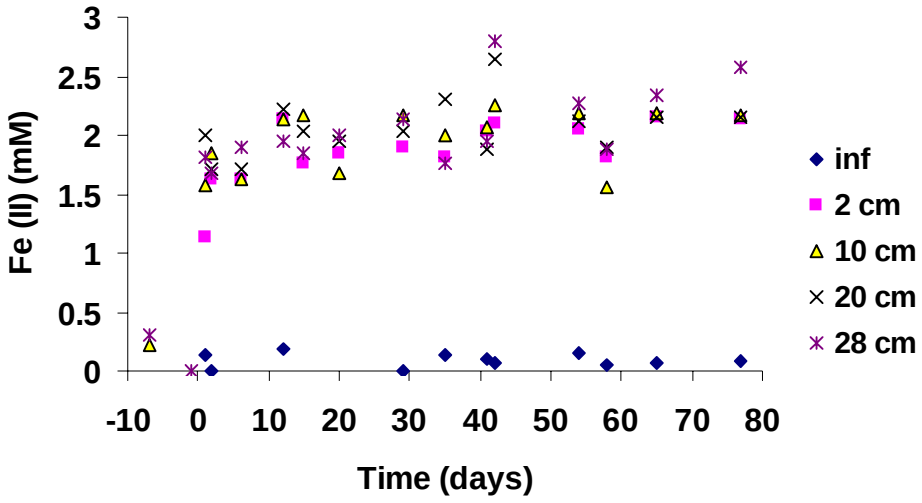

Figure 10. Fe(II) concentrations over time for different sampling ports located along the length of the 30 cm column

Steady values for Fe(II), acetate and H_2 were averaged for different sections of the 30 cm long column between day 40 and day 80 (Figure 11). A sharp rise in Fe(II) correlated with complete acetate oxidation by the first sampling port two cm into the column (Figure 11a). Additional iron reduction was observed along the remainder of the column, though to a lesser degree. Steady-state H_2 concentrations typical of iron-reducing conditions measured in the field (0.1-1 nM) were observed for the first 20cm of the column length (Figure 11b). Therefore, H_2 levels typical of ranges observed in the field during iron reduction are measured during the reduction of a soluble iron source (ferric citrate) when the carbon concentration is low (below the K_S^C).

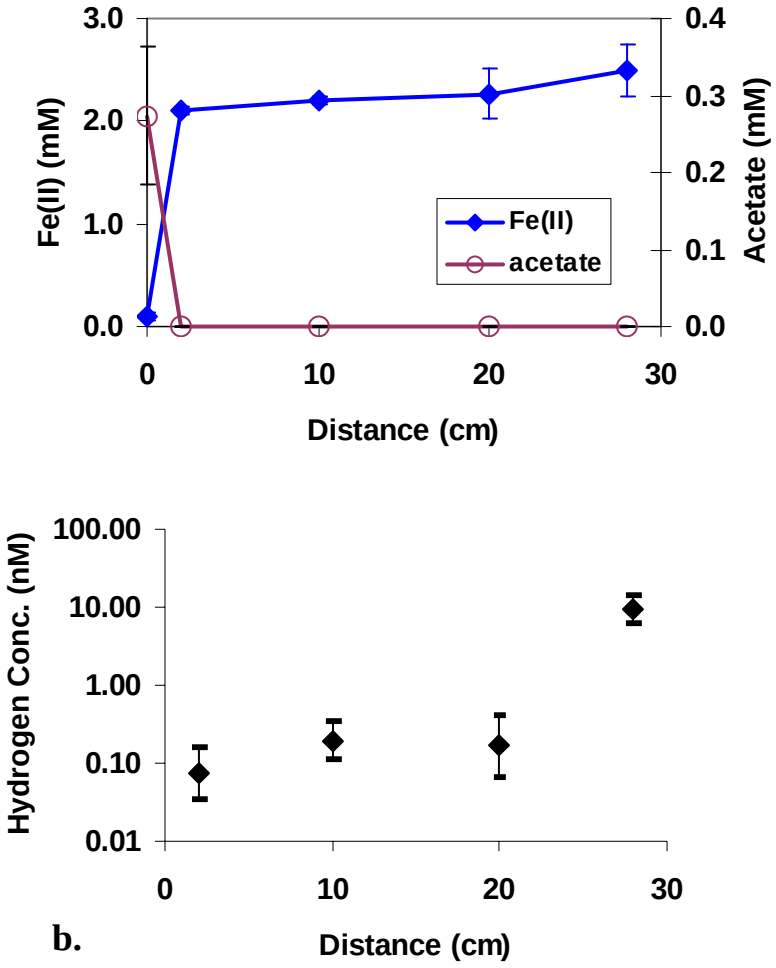

Figure 11. Steady-state a) Fe(II), acetate and b) H_2 concentrations measured during ferric citrate reduction. Initial Fe(III) concentrations was 5 mM.

Future Work

Column experiments will be performed using IOCS as the iron source to quantify the effect of carbon concentration on steady-state H_2 concentrations. The goal of this additional work is to determine if the dual-donor model developed in Phase 1 of this research can be used along with the kinetic coefficients for surface bound iron reduction measured from the IOCS batch experiments to predict steady-state H_2 concentrations during iron reduction. If so, this would imply that steady-state H_2 concentration ranges measured in the field are not only a function of the kinetics of the H_2 consuming organisms but also are impacted by the concentration of a co-electron donor, in this case a carbon source added as part of a biostimulation scenario for trace metal remediation.

Publications from this Research

- Komlos J. and P. R. Jaffé. 2004 "Effect of Iron Bioavailability on Dissolved Hydrogen Concentrations during Microbial Iron Reduction." *Biodegradation*, 15, pp. 315-325.

- Brown D.G., J. Komlos**,** and P. R. Jaffé. "Simultaneous Utilization of Acetate and Hydrogen by *Geobacter sulfurreducens* and Implications for Use of Hydrogen as an Indicator of Redox Conditions." *Environmental Science and Technology*, Status - In Review.

- Komlos, J., R.K. Kukkadapu, J.M. Zachara and P.R. Jaffé. "Quantification of Iron Oxidation in Microbially Reduced Sediment Containing Fe-oxide and Silicate Fe(II)/Fe(III) Minerals." Status - In Preparation.

- Komlos J. and P. R. Jaffé. "Influence of Co-Electron Donor Concentration and Iron Bioavailability on Hydrogen as an Indicator of Redox Conditions." Status - In Preparation.

Additional Presentations Involving this Research

- Komlos, J.**,** P.R. Jaffé, D.G. Brown and D.R. Lovley. "Hydrogen as an Indicator to Assess Biological Activity During Bioremediation Under Dual Electron Donor Conditions." 34th Mid-Atlantic Industrial and Hazardous Waste Conference, Cook College, Rutgers University, New Brunswick, NJ, September 20-21, 2002.

- Jaffé, P.R., J. Komlos, D.G. Brown and D.R. Lovley. "Hydrogen as an Indicator to Assess Biological Activity During Trace-Metal Bioremediation." AGU Spring Meeting, Washington, DC, May 28-31, 2002.

References

Ahring BK, Westermann P & Mah RA (1991) Hydrogen inhibition of acetate metabolism and kinetics of hydrogen consumption by *Methanosarcina-Thermophila* TM-1 Arch. Microbiol. 157: 38-42.

Anderson RT & Lovley DR (2002) In: Interactions of Microorganisms with Radionuclides; Keith-Roach, M. J., Livens, F. R., Eds.; Elsevier Science Ltd.

Anderson, RT, Vrionis HA, Ortiz-Bernad I, Resch CT, Long PE, Dayvault R, Karp K, Marutzky S, Metzler DR, Peacock A, White DC, Lowe M & Lovley DR (2003) Stimulating the in situ activity of *Geobacter* species to remove uranium from the groundwater of a uranium-contaminated aquifer. Appl. Environ. Microbiol. 69: 5884-5891.

Brown DG, Komlos J & Jaffe PR (2004) Simultaneous utilization of acetate and hydrogen by *Geobacter sulfurreducens* and the implications for use of hydrogen as an indicator of redox conditions. Environ. Sci. Technol. (in review)

Caccavo F, Lonergan DJ, Lovley DR, Davis M, Stolz JF & McInerney MJ (1994) *Geobacter sulfurreducens* sp. nov., a hydrogen- and acetate- oxidizing dissimilatory metal-reducing microorganism. Appl. Environ. Microbiol. 60: 3752-3759

Chapelle FH, McMahon PB, Dubrovsky NM, Fujii RF, Oaksford ET & Vroblesky DA (1995) Deducing the distribution of terminal electron-accepting processes in hydrologically diverse groundwater systems. Water Resour. Res. 31: 359-371

Chapelle F H, Haack SK, Adriaens P, Henry MA & Bradley PM (1996) Comparison of E_h and H_2 Measurements for Delineating Redox Processes in a Contaminated Aquifer. Environ. Sci. Technol. 30: 3565-3569

Chapelle FH, Vroblesky DA, Woodward JC & Lovley DR (1997) Practical considerations for measuring hydrogen concentrations in groundwater. Environ. Sci. Technol. 31: 2873-2877

Chapelle FH, Bradley PM, Lovley DR, O'Neill K & Landmeyer JE (2002) Rapid evolution of redox processes in a petroleum hydrocarbon-contaminated aquifer. Ground Water 40: 353-360

Hacherl EL, Kosson DS, Young LY & Cowan RM (2001) Measurement of iron(III) bioavailability in pure iron oxide minerals and soils using anthraquinone-2,6-disulfonate oxidation. Environ. Sci. Technol. 35: 4886-4893

Hoehler TM, Alperin MJ, Albert DB & Martens CS (1998) Thermodynamic control on hydrogen concentrations in anoxic sediments. Geochim. Cosmochim. Acta. 62: 1745-1756

Istok JD, Senko JM, Krumholz RL, Watson D, Bogle MA, Peacock A, Chang YJ & White DC (2004) *In Situ* Bioreduction of Technetium and Uranium in a Nitrate-Contaminated Aquifer. Environ. Sci. Technol. 38: 468-475

Löffler FE, Tiedje JM & Sanford RA (1999) Fraction of electrons consumed in electron acceptor reduction and hydrogen thresholds as indicators of halorespiratory physiology. Appl. Environ. Microbiol. 65: 4049-4056.

Lovley DR & Phillips EJP (1987) Competitive mechanisms for inhibition of sulfate reduction and methane production in the zone of ferric iron reduction in sediments. Appl. Environ. Microbiol. 53: 2636-2641

Lovley DR & Goodwin S **(**1988) Hydrogen concentrations as an indicator of the predominant terminal electron accepting reactions in aquatic sediments. Geochim. Cosmochim. Acta. 52: 2993-3003

Lovley DR, Chapelle FH & Woodward JC (1994) Use of dissolved H_2 concentrations to determine distribution of microbially catalyzed reactions in anoxic groundwater. Environ. Sci. Technol. 28: 1205-1210

Lovley DR (1995) Bioremediation of organic and metal contaminants with dissimilatory metal reduction. J. Indust. Microbiol. 14: 85-93.

Lovley DR, Coates JD, Blunt-Harris EL, Phillips EJP & Woodward JC (1996) Humic substances as electron acceptors for microbial respiration. Nature 382: 445-448

Lovley DR (2000) In *Environmental Metal-Microbe Interactions*; Lovley DR, Ed. ASM Press: Washington, DC

Liu C, Gorby YA, Zachara JM, Fredrickson JK, Brown CF (2002) Reduction kinetics of Fe(III), Co(III), U(VI), Cr(VI), Tc(VII) in cultures of dissimilatory metal reducing bacteria. Biotechnol. Bioeng. 80: 637-649

Madigan MT, Martinko JM, Parker J (1997) Brock: Biology of Microorganisms; 8th ed.; Prentice-Hall, Inc.: NJ.

Nevin KP & Lovley DR (2000) Potential for nonenzymatic reduction of Fe(III) via electron shuttling in subsurface sediments. Environ. Sci. Technol. 34: 2472-2478

Robinson JA & Tiedje JM (1984) Competition between sulfate-reducing and methanogenic bacteria for H_2 under resting and growing conditions. Arch. Microbiol. 137: 26-32.

Snoeyenbos-West OL, Nevin KP, Anderson RT & Lovley DR (2000) Enrichment of *Geobacter* species in response to stimulation of Fe(III) reduction in sandy aquifer sediments. Microb. Ecol. 39: 153-167.

Vroblesky DA, PM Bradley & FH Chapelle (1996) Influence of electron donor on the minimum sulfate concentration required for sulfate reduction in a petroleum hydrocarbon-contaminated aquifer. Environ. Sci. Technol. 30: 1377-1381

Watson IA, Oswald SE, Mayer KU, Wu Y & Banwart SA (2003) Modeling kinetic processes controlling hydrogen and acetate concentrations in an aquifer-derived microcosm. Environ. Sci. Technol. 37: 3910-3919

Wilhelm E, Battino R & Wilcock RJ (1977) Low-pressure solubility of gases in liquid water. Chem. Rev. 77: 219-262